

Low Reynolds Number Turbulent Boundary Layer Measurements

A.J. SMITS

Research Fellow in the Department of Mechanical Engineering, The University of Melbourne

V. BASKARAN

Post Graduate Student, Department of Mechanical Engineering, The University of Melbourne

L.P. ERM

Research Scientist, Division of Mechanical Engineering, Aeronautical Research Laboratories, Melbourne
and

P.N. JOUBERT

Professor of Mechanical Engineering, The University of Melbourne

SUMMARY The preliminary results of two experiments on low Reynolds number turbulent boundary layers are presented. The first experiment was a flat plate zero pressure gradient flow while the second experiment studied the flow over a two-dimensional circular arc profile of thickness-to-chord ratio 0.326. Both experiments showed discrepancies in the momentum integral balance which have not been satisfactorily resolved. The turbulence intensities on the flat plate displayed remarkable "inner" and "outer" flow scaling. The effects of pressure gradient and convex curvature on the circular arc profile had a strong effect on the turbulence intensities and no simple scaling could be discerned in this case.

1 INTRODUCTION

After transition from laminar to turbulent flow a turbulent boundary layer is considered to be a low Reynolds number flow until the Reynolds number based on momentum thickness R_θ is greater than approximately 5000. If the Reynolds number based on body length R_L is small the region where $R_\theta < 5000$ may be a significant part of the body length but no matter how high R_L becomes it is this part of the boundary layer which sets the initial condition for the subsequent layer development.

As a first step towards a better understanding of such flows an experimental study was made of a low Reynolds number turbulent boundary layer on a flat plate in a zero pressure gradient. The lack of turbulence measurements in such flows was seen as a further reason for initiating this study. An experimental study was concurrently made of the flow over a circular arc profile to investigate the effects of pressure gradient and longitudinal curvature. These two experiments are the first in a series of experiments specifically dealing with the behaviour of low Reynolds number flows and the preliminary results are presented in this report.

2 APPARATUS AND EXPERIMENTAL TECHNIQUE

2.1 Flat Plate

The flat plate formed the floor of a low-speed open-return wind tunnel. The working section was 2.5 m long with inlet dimensions 300 mm x 610 mm, and is described in detail by Fairlie (1973). The roof was adjusted so that a nominally zero pressure gradient was obtained. The pressure coefficient C_p , measured relative to an arbitrary reference, is given in figure 1(a).

To overcome the problem of probe access commonly encountered in low Reynolds number turbulent boundary layers the tunnel was run at a freestream velocity of approximately 5 m/s. With $R_\theta = 600$ this gave $\delta = 16.5$ mm, which is entirely adequate for turbulence measurements using crossed wires. To ensure that the boundary layer had a fixed origin a trip wire of 2.7 mm diameter was placed a few centimeters downstream of the contraction outlet. All measurements presented here were taken at distances greater than 68 diameters downstream of the trip wire, and all x distances were measured from the trip wire location. Mean flow

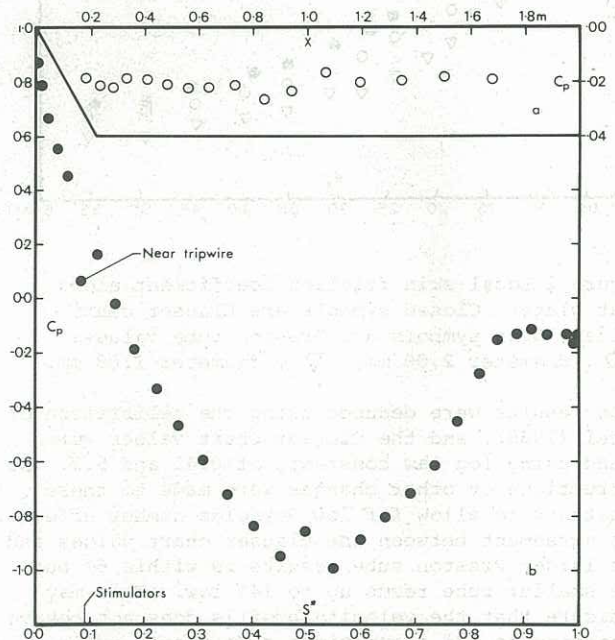


Figure 1 Distribution of pressure coefficient
(a) flat plate ○ (b) circular arc profile ●

measurements were taken with a flattened pitot tube of external dimensions 1.40 mm x 0.2 mm, in combination with a Barocel pressure transducer. Hot wire measurements were made with a constant temperature hot wire anemometer of Melbourne University design using a DISA 55P05 probe. All signal processing was carried out using an EAI Pace TR-20 analog computer. Static calibration techniques were used.

2.2 Circular Arc Profile

This work was carried out using the large wind tunnel in the Walter Bassett Laboratory of the Department of Mechanical Engineering. The working section is octagonal, measuring 1.68 m x 1.30 m with a length of 6.54 m. The model was a circular arc profile with a chord of 1.284 m and a thickness-to-chord ratio of 0.326. A trip wire 1.2 mm diameter was placed 110 mm downstream of the leading edge. The free stream velocity for all tests was maintained at 20.5 m/s giving $R_L = 1.69 \times 10^6$. Measurement techniques were similar to those used in the flat plate study, and further details of the

the tunnel and model are given in Smits and Baskaran (1980).

The pressure distribution is given in figure 1(b). The pressure recovery over the rear half of the profile leads to separation at approximately $s^* = 0.85$, where s^* is the coordinate along the surface non-dimensionalized by the total arc length.

3 RESULTS AND DISCUSSION

3.1 Flat Plate

The local skin friction coefficient C_f is plotted in figure 2 as a function of Reynolds number based on x , the distance from the trip wire. The Preston

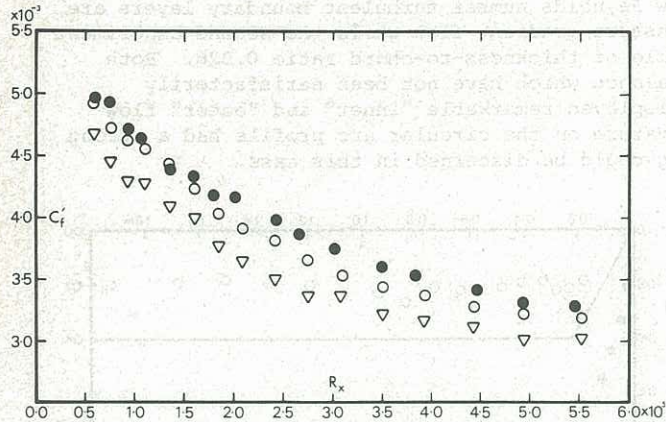


Figure 2 Local skin friction coefficient along flat plate. Closed symbols are Clauser chart values, open symbols are Preston tube values: \circ , diameter 2.00 mm; ∇ , diameter 1.08 mm.

tube results were deduced using the calibration of Patel (1965), and the Clauser chart values were found using log law constants of 0.41 and 5.2. No corrections or other changes were made to these constants to allow for low Reynolds number effects. The agreement between the Clauser chart values and the larger Preston tube results is within 6% but the smaller tube reads up to 14% low. This may indicate that the velocity profile does not behave according to the assumptions made above, or it may simply indicate that the Preston tubes are affected to some extent by viscous effects.

The displacement and momentum thicknesses, δ^* and θ , are shown in figure 3, as well as the shape factor H and R_θ . When the two-dimensional momentum integral balance was checked large discrepancies of the order of 60% were found. The flow was carefully checked with a yaw probe and the flow angle varied by less than 2° right across the tunnel, at the position $z = -150$ mm, $x = 1.2$ m. Spanwise skin friction measurements taken with a Preston tube varied by less than $\pm 3\%$ for $z = \pm 150$ mm at $x = .155$ m and 1.234 m. Large scale secondary flows are therefore ruled out as the source of the momentum imbalance.

The imbalance may be caused by an incorrect estimate of the skin friction coefficient. If the log law constants undergo a dramatic change as R_θ decreases Clauser chart and Preston tube methods may no longer be used. Huffman and Bradshaw (1972) suggested that this was unlikely. They found that the slope of the log law did not appear to be a function of Reynolds number, and

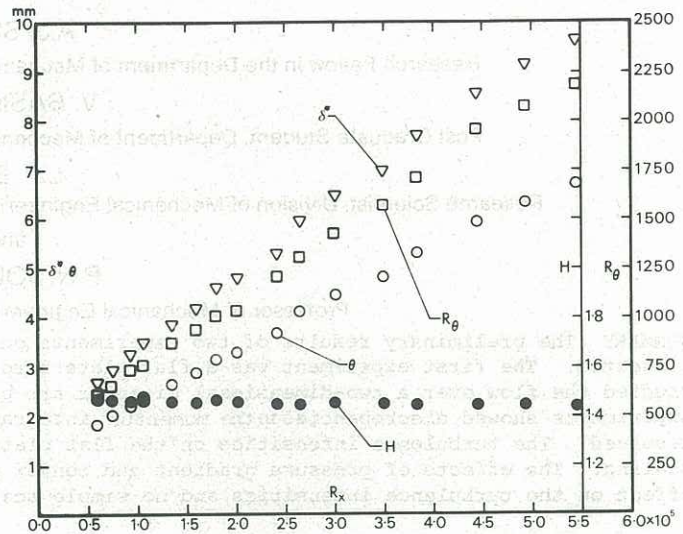


Figure 3 Integral parameters, flat plate.

that even the variation of the additive constant is likely to be small in boundary layers unless the influence of the outer layer is extremely large. In the present experiments R_θ varied from 600 to 2074. Possibly in this range of Reynolds numbers the strong viscous effects may affect the outer layer sufficiently to change the behaviour in the log law region. The recent measurements by Murlis (1975) indicate that this is unlikely to be the case.

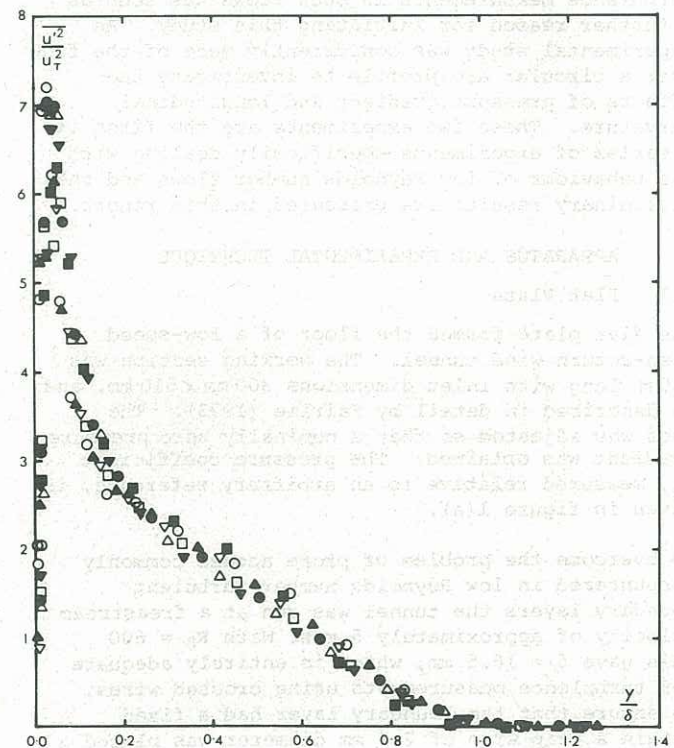


Figure 4 Longitudinal turbulence intensities for "outer" flow, flat plate: \blacksquare , $R_\theta = 600$; \blacktriangledown , 734; \triangle , 870; \bullet , 1006; \square , 1204; ∇ , 1421; \blacktriangle , 1701; \circ , 2074.

Longitudinal turbulence intensities $\overline{u'^2}$ are plotted in figures 4 and 5 using the friction velocity u_τ from the Clauser chart as the appropriate velocity scale. The "outer" flow data (figure 4) show a good collapse for $y/\delta > 0.1$ independent of R_θ , as suggested by Townsend's (1976) hypothesis of

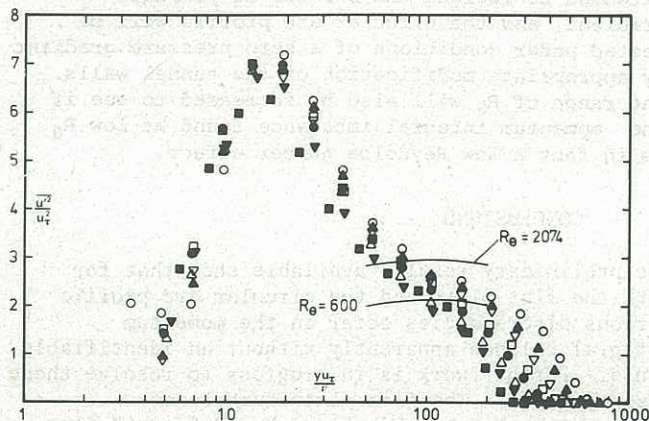


Figure 5 Longitudinal turbulence intensities for "inner" flow, flat plate. Symbols as for figure 4. Solid lines are predictions according to Henbest, Lim and Perry (1980).

Reynolds number similarity of the outer flow. That this should still hold at such low Reynolds numbers is indeed surprising.

For $y^+ < 100$ it can be seen from figure 5 that the turbulence intensities tend to collapse on a single curve using "inner" flow variables. A region of overlap between inner and outer flows does not appear in the present data since $y^+ = 100$ always exceeds $y/\delta < 0.1$. Nevertheless the predictions of Henbest, Lim and Perry (1980), which are only strictly valid in the overlap region show reasonable agreement with experiment.

3.2 Circular Arc Profile

To a first approximation, curvature effects are large when the ratio of boundary layer thickness δ to longitudinal radius of curvature R is large. Since the effect of curvature extra strain rates can be an order of magnitude larger than one would expect on the basis of the explicit terms appearing in the mean motion equations even small values of δ/R may have a significant effect (Bradshaw, 1973). From figure 6 it may be seen that the convex curvature of the circular arc profile is expected to have a noticeable effect on the boundary layer behaviour.

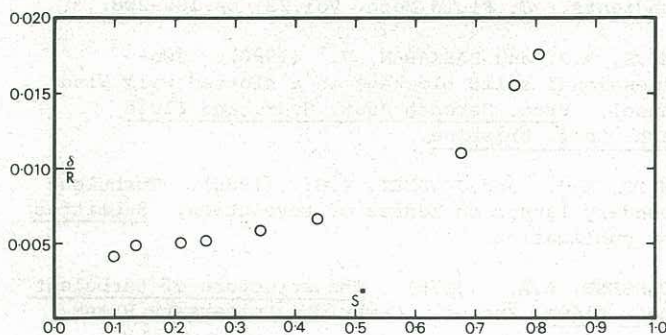


Figure 6 Ratio of boundary layer thickness to longitudinal radius of curvature, circular arc profile.

Local skin friction coefficients are shown in Fig.7 and the agreement between Clauser chart and Preston tube values is excellent. Predictions of C_f' using the calculation method of Bradshaw and Unsworth (1974) are consistently higher than the experimental values. This was also found to be the case for the four wings tested by Smits and Joubert (1980).

Figure 8 shows the integral parameters. Note that R_θ does not exceed 5000 until the point of separation is almost reached. A check of the

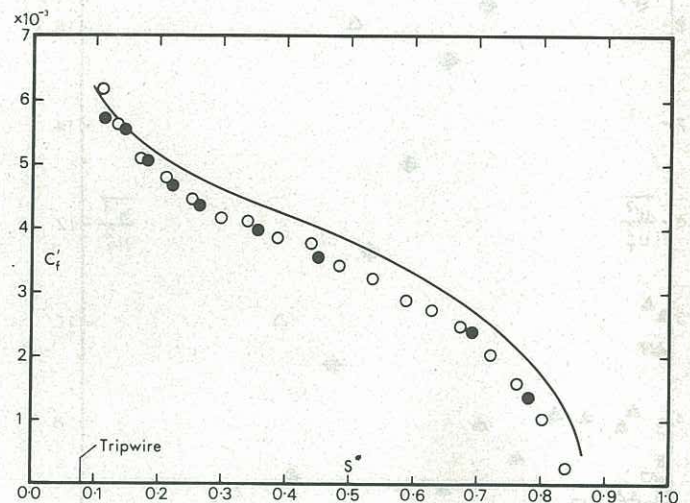


Figure 7 Local skin friction coefficients, circular arc profile. Open symbols are Preston tube values, closed symbols are Clauser chart values. Solid line is prediction according to Bradshaw and Unsworth (1974).

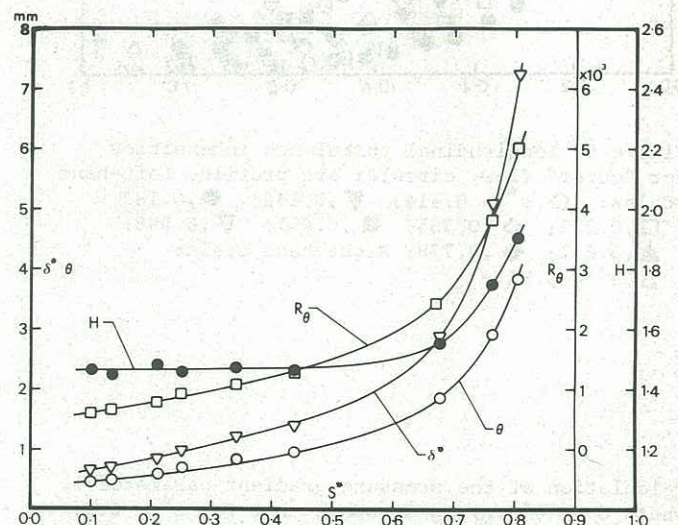


Figure 8 Integral parameters, circular arc profile.

momentum integral equation again showed large discrepancies, of the order of 30% in C_f' for $s^* < 0.7$. Approaching separation this discrepancy increased even further. Spanwise measurements of C_f' showed little evidence of significant secondary flows. The variation in C_f' at $s^* = 0.45$ was less than $\pm 2\%$ for $z = \pm 300$ mm, and the discrepancies observed in the momentum integral equation balance remain thus far unexplained.

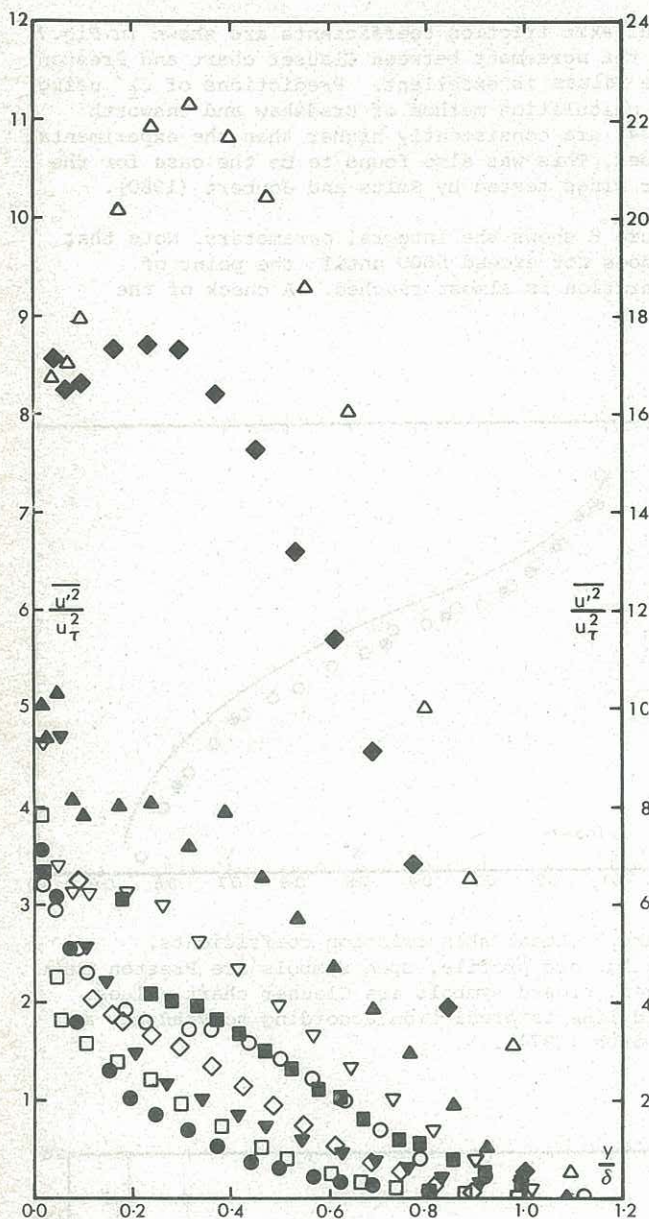


Figure 9 Longitudinal turbulence intensities for "outer" flow, circular arc profile. Left-hand scales: \circ , $s^* = 0.114$; ∇ , 0.146 ; \bullet , 0.183 ; \square , 0.222 ; \diamond , 0.355 ; \blacksquare , 0.451 ; \triangledown , 0.598 ; \blacktriangle , 0.691 ; \blacklozenge , 0.778 ; Right-hand scale: \triangle , $s^* = 0.817$.

Calculation of the pressure gradient parameter β , where $\beta = (\delta^*/\tau_w) dp/dx$ shows that for $s^* < 0.6$, β is constant and hence the flow is closely self-preserving. Figure 9, when contrasted with figure 4, demonstrates the dramatic effects of pressure gradients and longitudinal curvature on the behaviour of the longitudinal turbulence intensities. Except near the trip wire the trends seem to follow the pressure gradient. No measurements were taken in the separated region.

4 FUTURE WORK

The experiments described above are obviously only two scattered pieces of a particularly difficult jigsaw puzzle. In an effort to fill in some more of the picture, the flat plate study will be extended to include the effects of pressure gradient, and the circular arc profile will be tested under conditions of a zero pressure gradient by appropriate modification of the tunnel walls. The range of R_0 will also be increased to see if the momentum integral imbalance found at low R_0 is in fact a low Reynolds number effect.

5 CONCLUSIONS

The preliminary results available show that for both the flat plate and the circular arc profile serious discrepancies occur in the momentum integral balance apparently without an identifiable cause. Further work is in progress to resolve these discrepancies. The flat plate turbulence intensities clearly show "inner" and "outer" flow scaling, independent of R_0 , while the circular arc profile turbulence data suggests very strong effects of pressure gradient and convex curvature, although these two effects could not be separated. Work is proceeding towards that aim.

6 REFERENCES

- BRADSHAW, P. (1973) Effects of streamline curvature on turbulent flow. AGARDograph No.169.
- BRADSHAW, P. and UNSWORTH, K. (1974). An improved FORTRAN program for the Bradshaw-Ferriss-Atwell method of calculating turbulent shear layers. Aero. Rept. 74-03.
- FAIRLIE, B.D. (1973). A study of separation in turbulent boundary layers. Thesis (Ph.D.) University of Melbourne.
- HENBEST, S.M., LIM, K.L. and PERRY, A.E. (1980). The structure of turbulence in axisymmetric and flat plate flows. Proc. Seventh Aust. Hydr. and Fluid Mech. Conf. Brisbane.
- HUFFMAN, G.D. and BRADSHAW, P. (1972). A note on von Kármán's constant in low Reynolds number turbulent flows. J. Fluid Mech. Vol.53, pp.54-60.
- MURLIS, J. (1975). Turbulence at low Reynolds number. Thesis (Ph.D.) Imperial College, London.
- PATEL, V.C. (1965). Calibration of the Preston tube and limitations on its use in pressure gradients. J. Fluid Mech. Vol.23, pp.185-208.
- SMITS, A.J. and BASKARAN, V. (1980). Two-dimensional solid blockage in a slotted wall wind tunnel. Proc. Seventh Aust. Hydr. and Fluid Mech. Conf. Brisbane.
- SMITS, A.J. and JOUBERT, P.N. (1980). Turbulent boundary layers on bodies of revolution. Submitted for publication.
- TOWNSEND, A.A. (1976). The structure of turbulent shear flows. 2nd ed., Cambridge University Press.